

Structure-Function Studies of Bacteriorhodopsin XV

EFFECTS OF DELETIONS IN LOOPS B-C AND E-F ON BACTERIORHODOPSIN CHROMOPHORE AND STRUCTURE*

(Received for publication, November 15, 1990)

Marie A. Gilles-Gonzalez^{‡§}, Donald M. Engelman[¶], and H. Gobind Khorana[‡]

From the [‡]Departments of Biology and Chemistry, Massachusetts Institute of Technology, Cambridge, Massachusetts 02139 and the [¶]Department of Molecular Biophysics and Biochemistry, Yale University, New Haven, Connecticut 06511

Bacteriorhodopsin mutants containing deletions in loop B-C, Δ Thr⁶⁷-Glu⁷⁴ or Δ Gly⁶⁵-Gln⁷⁵, or a deletion in the loop E-F, Δ Glu¹⁶¹-Ala¹⁶⁸, were prepared. Following their expression in *Escherichia coli*, the mutant proteins were purified to homogeneity and refolded with retinal in detergent-phospholipid mixtures. The mutants containing deletions in the loop B-C were normal at 4 °C but showed the following changes at 20 °C. 1) The λ_{\max} shifted from 540 to below 510 nm; 2) the rates of bleaching by hydroxylamine in the dark increased; and 3) the rate and steady state of proton pumping decreased. Deletion of the eight amino acids in loop E-F did not affect wild-type behavior. However, all the mutant proteins were more prone to thermal and sodium dodecyl sulfate denaturation than the wild-type bacteriorhodopsin. These observations show that the structures of the B-C and E-F loops are not essential for correct folding of bacteriorhodopsin, but they contribute to the stability of the folded protein.

various models proposed (6-9), and photoaffinity labeling experiments have indicated that E-F is also a large loop (7). In the present work we examine the effects of deletions in the loops on the folding, function, and stability of bR. Deletions of amino acids Thr⁶⁷-Glu⁷⁴ and Gly⁶⁵-Gln⁷⁵ in the loop connecting helices B and C were made and of amino acids Glu¹⁶¹-Ala¹⁶⁸ in the loop between helices E and F. The B-C loop lies on the extracellular side of the membrane and the E-F loop on the cytoplasmic side.

We found that all the deletions destabilize the structure to some extent, as measured by sensitivity to thermal and SDS denaturation. No effect was seen on proton pumping and the absorption spectrum in the case of the E-F deletion; however, the two deletions in loop B-C show blue shifts in the chromophore absorption maximum, diminished proton pumping, and increased susceptibility to hydroxylamine bleaching. In all cases, the basic folding of bR occurs as judged by circular dichroism, chromophore binding, and proton pumping.

EXPERIMENTAL PROCEDURES

Materials

T4 DNA ligase was purified from *Escherichia coli* lysogenized with phage λ expressing T4 ligase (10). Restriction endonucleases were from New England Biolabs and Boehringer Mannheim. The Klenow fragment of *E. coli* DNA polymerase I was purchased from Bethesda Research Laboratories. The "slow" form of nuclease Bal-31 was obtained from International Biotechnologies, Inc. Radiolabeled nucleotides were purchased from Amersham Corp. Nitrocellulose BA85 filter was from Schleicher and Schuell. Media for the growth of bacteria were supplied by Difco. DEAE-Trisacryl was obtained from LKB. Octyl glucoside and CHAPS were from Behring Diagnostics; DMPC was from Avanti Polar Lipids, Inc. Nucleotides, ampicillin, Nonidet P-40, phenylmethylsulfonyl fluoride, lysozyme, antifoam C, and RNase A were obtained from Sigma. All-*trans* retinal and 13-*cis* retinal were from Kodak.

Methods

General Recombinant DNA Methods—Digestions with restriction enzymes were performed as recommended by Fuchs and Blakesley (11) or by the commercial suppliers of the endonucleases. Both small- and large-scale plasmid preparations were done by alkaline sodium dodecyl sulfate lysis procedures (12, 13). In large-scale preparations, plasmid DNA was purified by equilibrium centrifugation in cesium chloride gradients containing ethidium bromide and by gel filtration on Bio-Gel A-50m. Restriction digestions were monitored on 0.6-1.7% agarose gels containing 0.5 μ g/ml of ethidium bromide. Restriction fragments for ligations were purified from SeaPlaque-agarose gels (14).

Construction of Deletions in *bop* Gene—The pXB/Gal 101 plasmid (15) was digested with either *Kpn*I or *Sph*I to completion. An aliquot of DNA (1 μ g) was treated with 0.16 units of slow Bal-31 in 10 μ l of 20 mM Tris-HCl (pH 8.0), 0.6 M NaCl, 12.5 mM MgCl₂, and 12.5 mM CaCl₂ at 0 °C for 15-60 s. The reaction was stopped with 0.1 M EDTA. Pure DNA was recovered and treated with the Klenow fragment of DNA polymerase I, in the presence of all four deoxynucleotide tri-

Bacteriorhodopsin (bR),¹ an integral membrane protein in *Halobacterium halobium*, serves as a light-dependent proton pump (1). It consists of a single polypeptide chain of 248 amino acids and contains the chromophore all-*trans* retinal, linked via a Schiff base to lysine 216 (2-5). The model shown in Fig. 1 is based mainly on electron microscopy, with contributions from neutron diffraction, proteolysis studies, and photoaffinity labeling (9). Some uncertainty remains regarding the sizes of embedded helices and of the loops connecting the different helices. Loop B-C has been consistently large in

* This work was supported by Grants GM28289 and AI 11479 from the National Institutes of Health and Grant N00014-82-K-0668 from the Office of Naval Research, Department of the Navy (to H. G. K.) and by National Science Foundation Grant DMB 8805587 and National Institutes of Health Grant 5 P01 GM 22778 (to D. E.). The costs of publication of this article were defrayed in part by the payment of page charges. This article must therefore be hereby marked "advertisement" in accordance with 18 U.S.C. Section 1734 solely to indicate this fact.

§ Current address: University of California, San Diego, CA 92093.

¹ The abbreviations used are: bR, bacteriorhodopsin; *bop*, bacteriorhodopsin gene with native sequence; *bop:lacZ*, in-frame translational fusion of the nearly complete *bop* gene upstream to the *E. coli lacZ* gene, which yields a fusion protein with β -galactosidase activity; bO, bacterio-opsin; ebO, bacterio-opsin as obtained by expression of the *bop* gene and purified *in vitro*; eBR, bacteriorhodopsin obtained by regeneration of ebO *in vitro*; DMPC, L- α -dimyristoylphosphatidylcholine; CHAPS, 3-[(3-cholamidopropyl)dimethylammonio]-1-propanesulfonate; SDS, sodium dodecyl sulfate; Δ Thr⁶⁷-Glu⁷⁴, a deletion of the eight ebO residues including threonine 67 to glutamate 74; Δ Gly⁶⁵-Gln⁷⁵, a deletion of the eleven ebO residues including glycine 65 to glutamine 75; Δ Glu¹⁶¹-Ala¹⁶⁸, a deletion of the eight ebO residues including glutamate 161 to alanine 168.

phosphates, and then treated with T4 DNA ligase. The ligation mixture was used directly to transform the *E. coli* Δlac strain LG90 by the procedure of Hanahan (16, 17). The transformants were initially screened after 16 h of growth at 37 °C on lactose McConkey plates supplemented with ampicillin (35 $\mu\text{g}/\text{ml}$). Plasmids from *lac*⁺ colonies were tested for the absence of *Kpn*I or *Sph*I sites. The size of each deletion was determined by further restriction analysis of plasmid DNA from each *lac*⁺ clone and demonstration of the changed electrophoretic mobilities of two *bop* *Ava*II fragments. The loop B-C deletions were transferred to M13 and sequenced by the dideoxy chain termination method (18). The loop E-F in-frame deletions were sequenced directly from double-stranded plasmid DNA (18, 19).

Expression, Purification, and Immunological Identification of ebO Deletion Mutants—*E. coli* C600 (p1857) strain (20) was transformed with the pPLB05-CT Δ vectors (Fig. 2). Expression of the ebO mutants by temperature induction, their solvent extraction, and DEAE-Trisacryl purification were done as described previously for ebO (21, 22). The purified proteins (2 mg/ml) were dissolved in 1% SDS (w/v) and stored at -20 °C as lyophilized powders of these solutions. Immunodetection was essentially as described (21).

UV-visible Absorbance Measurements and Protein Determination—UV-visible spectra were taken on a Beckman DU-7 or Perkin-Elmer Lambda 7 spectrophotometer in 1-cm path length quartz cells. The temperature was controlled to within 0.1 °C with jacketed cell holders connected to a circulating bath (NESLAB, ENDOCAL). Retinal concentrations were based on molar extinctions of 43,000 for all-trans retinal and 35,000 M⁻¹ cm⁻¹ for 13-cis retinal in absolute ethanol at 380 nm. Protein concentration was based on 280-nm extinction coefficients of 66,000 M⁻¹ cm⁻¹ for ebO in SDS and 79,000 M⁻¹ cm⁻¹ in DMPC/CHAPS/SDS at pH 6.0 (23). Extinction coefficients for the chromophores of the mutants were calculated from the initial slopes of the retinal binding curves of the proteins (24). The chromophores of $\Delta\text{Thr}^{67}\text{-Glu}^{74}$ and $\Delta\text{Gly}^{65}\text{-Gln}^{75}$ had an extinction of 41,000 M⁻¹ cm⁻¹ at 490 nm in DMPC/CHAPS/SDS at pH 6.0. $\Delta\text{Glu}^{161}\text{-Ala}^{168}$ and eBR had 550-nm extinctions of 59,000 and 52,000 M⁻¹ cm⁻¹, respectively, in DMPC/CHAPS/SDS at pH 6.0.

Circular Dichroism Measurements—Reconstitution of the mutants was essentially as described, with minor modifications to accommodate their instability (25). Protein (0.8 mg) was dissolved in 1.0 ml of 5.0% SDS and 1.5 mM NaP_i (pH 6.0). An equal volume of the same buffer containing 0.08% taurocholate, 0.08% *H. halobium* lipids, and 1.5 M eq of 13-cis retinal was added, in the dark. Potassium chloride (103 μl of a 4.0 M solution) was added slowly to the sample, in order to precipitate the dodecyl sulfate, and the protein was recovered in the supernatant after 30 min by centrifugation. The vesicles thus produced were immediately dialyzed (Spectra Por membrane, 12–14 kDa cutoff), in the dark, against 500 volumes of 150 mM KCl, 50 mM KP_i (pH 6.0) at 4 °C (three changes, 3 days).

CD spectra were recorded with an AVIV 60DS spectropolarimeter interfaced with an IBM personal computer containing the appropriate software. The sample holder was a water-jacketed cylindrical cell with a 1-mm path length. Its temperature was controlled to 0.1 °C by a circulating bath (NESLAB ENDOCAL, model RTE.4DD) and was monitored directly with a thermocouple (Bailey Instruments, Inc.). The temperature was increased in steps of 5–6 °C, allowing ample time for equilibration between measurements. Data points were taken every 1 nm. The sample consisted of 0.1–0.2 mg/ml of protein reconstituted in *H. halobium*-lipid vesicles; the reference consisted of the final buffer against which the vesicles had been dialyzed. The average of three reference spectra was subtracted from the average of three uncorrected spectra taken at the same temperature, to give the curves from which the 222-nm values were obtained.

Reconstitution and Proton Pumping—Protein was reconstituted in soybean lipid vesicles essentially as described earlier (1, 22), except that after regeneration in the dark for 16 h, dodecyl sulfate was removed by precipitation with equimolar KCl and centrifugation (25). Standard assays of proton pumping used a 25-fold dilution of the vesicle preparation into 2 M NaCl equilibrated at 30 °C and blanketed with argon (1, 22). For studies of the temperature dependence of proton pumping, the dilution solution was 0.1 mM NaP_i (pH 6.0) at 4 °C. Measurements were made after bringing the samples from 4 °C to the desired temperature and allowing them to equilibrate. The light source was a 250-watt lamp from a Kodak slide projector, focused on the reaction vessel, without any filter. After each measurement, the recorder was calibrated with a small volume of 1 mM HCl (1–5 μl for standard assay mixtures, 10–30 μl for buffered mixtures). The amount of protein in the calculations of protons pumped was based on regenerated chromophore rather than total protein.

SDS Denaturation—The kinetics of SDS denaturation were determined by mixing, in the dark, 250 μl of a regeneration mixture (26) pre-equilibrated at 20 °C and 75 μl of 10% SDS (w/v). The sample was quickly inverted three to four times, and recording of its 250–750-nm UV-visible spectrum was begun within 30 s. During the first 5 min of the denaturation, spectra were taken at 1-min intervals. Then the spectra were recorded less frequently, until only the absorbance of retinal remained, near 385 nm.

For equilibrium studies of the extent of denaturation in varying concentrations of SDS, 125- μl aliquots of regeneration mixture (26) were mixed in the dark with solutions of SDS, calculated to give final SDS concentrations ranging from 0.1 to 4.0% in a total volume of 250 μl . They were allowed to equilibrate 20–24 h at 30 °C, in the dark, and their dark-adapted UV-visible spectra were recorded the following day.

Hydroxylamine Bleaching of Regenerated ebO Mutants—Hydroxylamine hydrochloride (pH 6.0) was added to a final concentration of 0.1 M to a quartz cuvette containing regeneration mixture prepared as described previously (26). The samples were equilibrated at each temperature in the spectrophotometer chamber, in the dark. Scans (250–750 nm) lasting 25 s or less were taken at the indicated times after addition of hydroxylamine.

RESULTS

Production of *bop* Deletion Mutants

We aimed to delete only portions of the amino acids presumed to be in the loops B-C and E-F of bO without introducing new amino acid changes (Fig. 1). Our strategy was to cut the plasmid carrying a *bop:lacZ* gene fusion (Fig. 2) at restriction sites *Kpn*I or *Sph*I, corresponding to loops B-C and E-F, respectively. The cuts were extended on both sides by limited treatment with Bal-31 exonuclease at 0 °C, and the DNA was religated. We screened for in-frame deletions of the appropriate size in three steps, as follows. 1) We transformed an *E. coli* Δlac strain with the mutated plasmids, expecting in-frame *lac*⁺ clones at a frequency of 33%. 2) We checked that *lac*⁺ clones had lost the *Kpn*I or *Sph*I site, to distinguish in-frame deletions from parentals. 3) We estimated the sizes of the deletions from the altered mobilities of two *bop* *Ava*II fragments on sequencing gels. Ten percent, rather than 33% of the transformants were *lac*⁺. It is possible that the remaining molecules were merely blunt-ended by mild exonuclease treatment and religated out of frame. Virtually no parentals were found, and approximately 40% of the clones had dele-

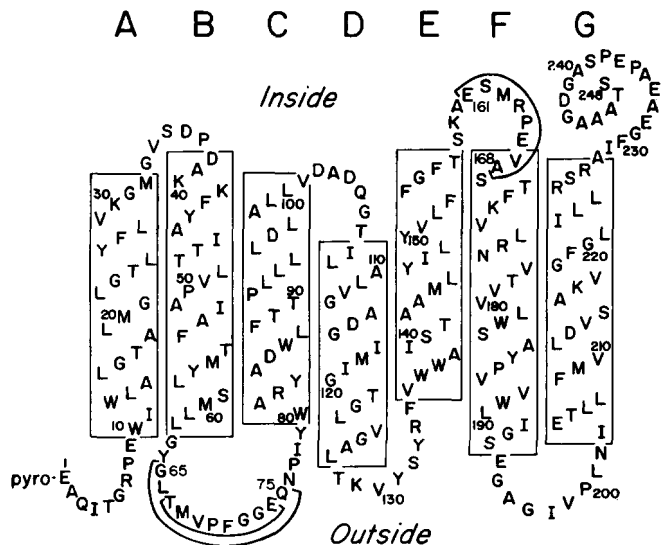


FIG. 1. A secondary structure model for bacteriorhodopsin. The seven helices embedded in the membrane are designated by letters A-G. The amino acids deleted in loops B-C and E-F are indicated by solid lines.

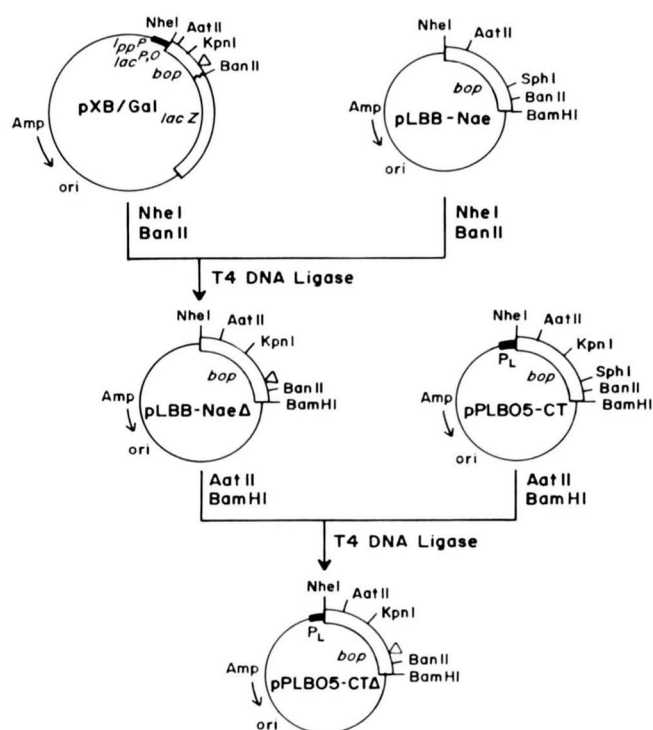


FIG. 2. Scheme for transferring the deletions made in the *bop* gene into plasmid pLBO5-CT (21) for temperature-inducible expression. The *Sph*I and *Kpn*I sites in the native *bop* gene are in sequences encoding loop E-F and loop B-C, respectively. The scheme is shown here for deletions in the loop E-F.

tions of 20 or fewer codons. In all, we obtained 79 clones with in-frame deletions in loops B-C and E-F. The smallest loop B-C deletions were cloned into M13, and the entire insert, including the region from *Aat*II to *Sph*I (Fig. 2), was sequenced. The sequence information obtained for the loop E-F mutants covered the region from *Aat*II to *Ban*II (Fig. 2). We chose the three mutants in this study for their small size and the lack of codon changes at the deletions' boundaries. They are: Δ Thr⁶⁷-Glu⁷⁴ and Δ Gly⁶⁵-Gln⁷⁵ in extracytoplasmic loop B-C and Δ Glu¹⁶¹-Ala¹⁶⁸ in cytoplasmic loop E-F.

Temperature-inducible Production of the Mutated Proteins

The deletion mutations in *bop* were transferred unidirectionally to the expression vector pLBO5-CT (21), downstream of the λ P₁ promoter (Fig. 2). Since the pXB/Gal 101 plasmid (15) lacks suitable unique sites for transfer of the *bop* gene, a smaller vector, pLBB-Nae, was constructed with unique *Nhe*I and *Ban*II sites. The subsequent construction of pLBO5-CT Δ is shown in Fig. 2. For *bop* expression, the λ cI857 temperature-sensitive repressor was provided in *trans* so that induction could be carried out by a temperature shift.

Characterization of the Bacteriorhodopsin Deletion Mutants

Electrophoretic Mobilities and Immunoblotting—The purified mutant ebO's were identified by Western blot analysis, using the monoclonal antibody BR114, specific for the bR carboxyl terminus (27). The increased electrophoretic mobility of the mutated proteins further confirmed the deletions (Fig. 3). The yield of purified protein was about 0.1 mg/g of wet *E. coli* cells in all cases.

Rates of Chromophore Regeneration—All the mutated proteins folded, bound retinal, and regenerated bR-like chromophores. Regeneration, on the whole, was slower (Fig. 4). The half-times of regeneration for ebR, Δ Thr⁶⁷-Glu⁷⁴, Δ Gly⁶⁵-

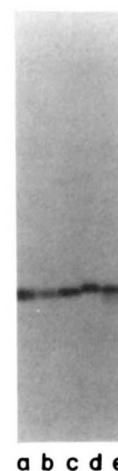


FIG. 3. Immunological detection of purified mutant bacterio-opsins containing deletions. The mutant genes (Fig. 2) were expressed in *E. coli* strain C600 (pCI857) after their induction at 42 °C. The proteins were purified and subjected to SDS gel electrophoresis. All the ebO-related proteins (0.5–1 μ g each) were detected with the monoclonal antibody BR114. The lanes show: Δ Glu¹⁶¹-Ala¹⁶⁸ (lane a); Δ Gly⁶⁵-Gln⁷⁵ (lane b); Δ Thr⁶⁷-Glu⁷⁴ (lane c); ebO (lane d); and purple membrane (lane e).

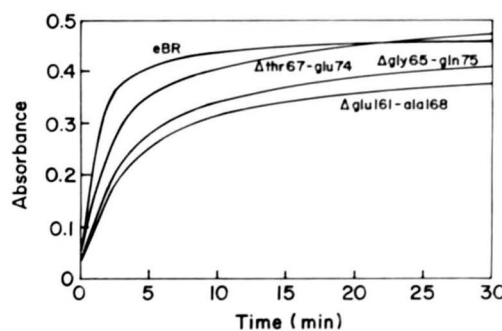


FIG. 4. Time course of regeneration of the native ebR and the deletion mutants. Regeneration of the opsins was carried out in a solution of 50 mM NaP_i (pH 6.0), DMPC (2% w/v), CHAPS (0.75% w/v), and SDS (0.2% w/v) using a 10-fold molar excess of all-*trans* retinal (26). Measurement of the absorbance at λ_{max} was begun within 30 s after mixing the assay components with the proteins.

Gln⁷⁵, and Δ Glu¹⁶¹-Ala¹⁶⁸, measured at their wavelength of maximal absorption at 20 °C, were, respectively 84, 120, 150, and 210 s with all-*trans* retinal. The extent of regeneration varied, being 76, 60, 73, and 52% for ebO, Δ Thr⁶⁷-Glu⁷⁴, Δ Gly⁶⁵-Gln⁷⁵, and Δ Glu¹⁶¹-Ala¹⁶⁸, respectively.

UV/Visible Absorption Characteristics—The deletion mutant Δ Glu¹⁶¹-Ala¹⁶⁸, following regeneration, was like ebR (Fig. 5B) (22). Its chromophore showed normal light-dark adaptation (shift from 554 to 560 nm). The absorption characteristics were unaffected by temperature, changing less than 2 nm as the temperature was increased from 4 to 30 °C (Fig. 6D).

The mutants Δ Gly⁶⁵-Gln⁷⁵ (Fig. 5A) and Δ Thr⁶⁷-Glu⁷⁴ showed little or no light adaptation, and the absorption of their chromophore was very dependent on temperature (Fig. 6D). The dark-adapted chromophore absorptions were 541 and 533 nm, respectively, for mutants Δ Thr⁶⁷-Glu⁷⁴ and Δ Gly⁶⁵-Gln⁷⁵ at 4 °C. As the temperature was raised to 30 °C, their absorption broadened and shifted toward shorter wavelengths by more than 30 nm (Fig. 6D). The temperature effects were completely reversible for both mutants at up to 50 °C.

Thermal Denaturation, as Measured by Changes in Circular Dichroism—Large negative ellipticity at 208 and 222 nm in

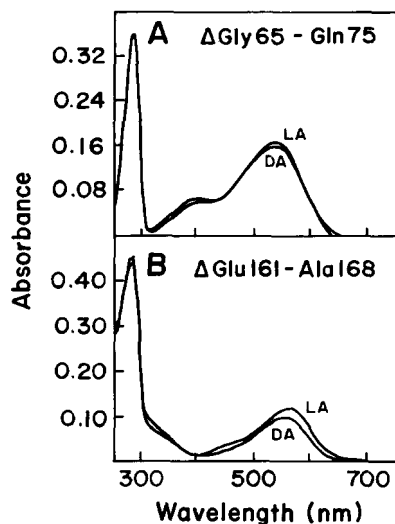


FIG. 5. Light-dark adaptation of deletion mutants. Loop B-C mutant Δ Gly⁶⁵-Gln⁷⁵ (A) and loop E-F mutant Δ Glu¹⁶¹-Ala¹⁶⁸ (B) were each regenerated with equimolar amounts of all-*trans* retinal as described in the legend to Fig. 4. Dark-adapted spectra (DA) were from samples equilibrated in the dark for 24 h. Light-adapted (LA) spectra were from the same samples after 10 min of illumination with a 300-watt projector lamp. All the spectra were recorded at 4 °C.

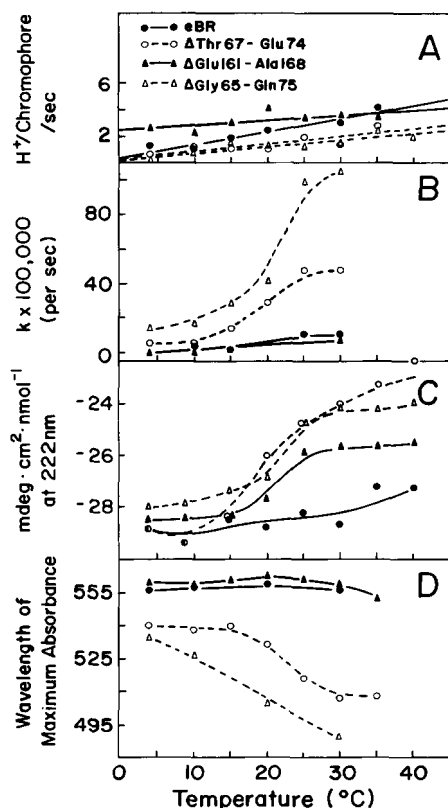


FIG. 6. Temperature stability of ebR and the deletion mutants. The temperature of the regenerated samples was gradually increased from 4 °C. The samples were equilibrated for 10–20 min at each temperature prior to each measurement. A, dependence of proton translocation on temperature; B, effect of temperature on hydroxylamine denaturation kinetics; C, effect of temperature on secondary structure; D, effect of temperature on wavelength of absorption. Details are described under “Methods.”

the CD spectra indicated substantial α -helicity for ebR and the deletion proteins. The 222-nm values of spectra taken over a temperature of 4–40 °C obeyed the shape of a melting curve, with a midpoint temperature (T_m) value close to 22 °C

for all three mutants (Fig. 6C). This transition was completely reversed on cooling. During heating, the negative ellipticity of the mutated proteins decreased more than ebR, indicating some loss of secondary structure (Fig. 6C). These thermal effects agreed well with the results of thermal denaturation monitored for the loop B-C mutants by UV-visible spectroscopy (Fig. 6D).

Proton Pumping after Reconstitution in Vesicles— Δ Glu¹⁶¹-Ala¹⁶⁸ pumped protons like ebR. The initial rate of pumping was 3–5 H⁺/chromophore/s, and the steady-state level pumped was 30–50 H⁺/chromophore, under the standard conditions (Fig. 7) (22). Temperature dependence effects were studied under the conditions described under “Methods.” We obtained initial rates comparable with those measured under the standard conditions (the steady-state levels rose approximately 10-fold for each protein). Δ Glu¹⁶¹-Ala¹⁶⁸ functioned as well as or better than ebR over the entire range of 4–35 °C (Fig. 6A).

Δ Thr⁶⁷-Glu⁷⁴ and Δ Gly⁶⁵-Gln⁷⁵ pumped protons at initial rates 10 times lower and plateau levels three times less than ebR, under the standard conditions (Fig. 7). In contrast to the loop E-F mutant, temperatures exceeding 15 °C caused a reduction in these mutants’ initial rates of pumping (Fig. 6A).

Denaturation in Sodium Dodecyl Sulfate—The course of the denaturation was followed spectroscopically after adding 2.5% SDS (w/v) to protein which had been regenerated in DMPC/CHAPS/SDS micelles. At 20 °C, a denaturation intermediate at 600 nm and another at 440 nm were readily observed for ebR before the release of free retinal (Fig. 8). The 600-nm intermediate appeared first and decayed into the

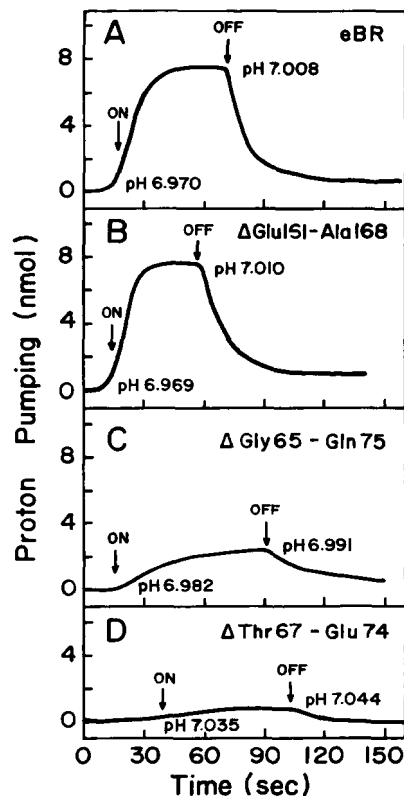


FIG. 7. Light-dependent proton pumping by ebR and the deletion mutants. ebR (163 pmol) (A), 163 pmol of Δ Glu¹⁶¹-Ala¹⁶⁸ (B), 199 pmol of Δ Gly⁶⁵-Gln⁷⁵ (C), and 83 pmol Δ Thr⁶⁷-Glu⁷⁴ (D) were reconstituted in soybean-lipid vesicles as described under “Methods.” Assays were at 30 °C in 2 M NaCl blanketed with argon. Alkalinization of the medium upon illumination was followed with a microelectrode. Illumination is indicated by the “ON” arrow. Cessation of illumination is indicated by the “OFF” arrow.

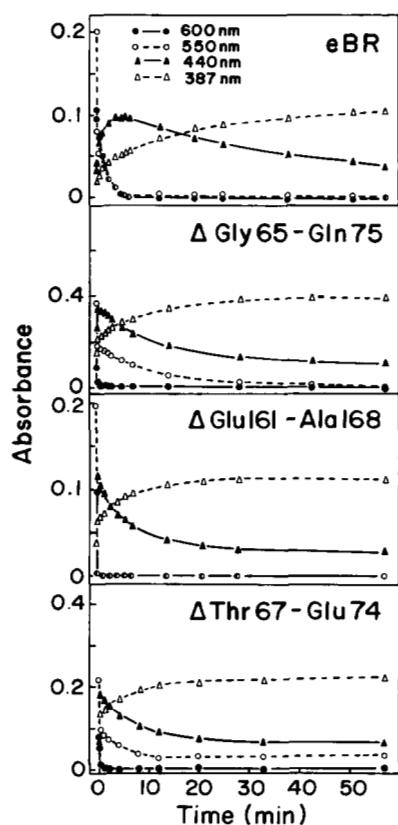


FIG. 8. Kinetics of denaturation of ebR and the deletion mutants by SDS. ebR (A), Δ Gly⁶⁵-Gln⁷⁵ (B), Δ Glu¹⁶¹-Ala¹⁶⁸ (C), or Δ Thr⁶⁷-Glu⁷⁴ (D) were regenerated with 1 M eq of all-*trans* retinal, as described in the legend to Fig. 4. Following addition of SDS (2.5% w/v), each solution was quickly mixed, and its spectra were taken at varying times, starting at 15 s.

440-nm species with a $t_{1/2}$ of 2 min. For early spectra, an isobestic point could be seen at 490 nm. The disappearance of the 440-nm species left only the absorbance of free retinal. In sharp contrast to the wild-type behavior, all of the deletion mutants immediately denatured to the 440-nm species without the 600-nm transition (Fig. 8). Free retinal was released directly from their shorter-lived 440-nm species, with an isobestic point at 420 nm.

The general stabilities of the ebR mutants were also compared by their extents of denaturation at equilibrium (16 h of incubation) in concentrations of SDS ranging from 0.1 to 4.0% (w/v). ebR was more stable to SDS than any of the mutants (Fig. 9). Their order of stability, determined by the SDS concentrations at which half of the original chromophore remained, was ebR (1.9%) > Δ Thr⁶⁷-Glu⁷⁴ (1.4%) > Δ Gly⁶⁵-Gln⁷⁵ (1.1%) > Δ Glu¹⁶¹-Ala¹⁶⁸ (0.78%) (Fig. 9).

Bleaching by Hydroxylamine—Irradiation is required to render the Schiff base of bR accessible to water-soluble reagents like hydroxylamine (28). We followed the reaction of the Schiff base of the mutants with hydroxylamine in the dark as a measure of the integrity of their chromophores' environment. Hydroxylamine did not significantly bleach ebR in the dark, and mutant Δ Glu¹⁶¹-Ala¹⁶⁸ behaved identically to ebR (Fig. 6B). Rates of bleaching four to ten times higher were observed for Δ Thr⁶⁷-Glu⁷⁴ or Δ Gly⁶⁵-Gln⁷⁵ at 30 °C. The activation energies for this transition were +14.6 kcal/mol for Δ Thr⁶⁷-Glu⁷⁴ and +16.5 kcal/mol for Δ Gly⁶⁵-Gln⁷⁵ (obtained from the Arrhenius relation $\ln k = (-E_a/R) 1/T + \ln A$, where k is the rate constant obtained at temperature T , T is the temperature in Kelvin degrees, $R = 1.987$ cal/mol·K, and A is also a constant).

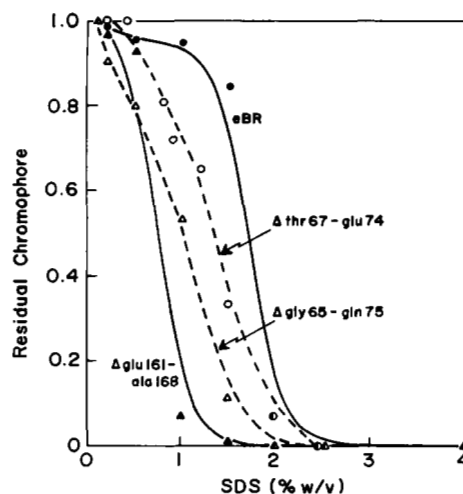


FIG. 9. Stability of ebR and the deletion mutants to increasing concentrations of SDS. Varying amounts of SDS were added to the samples that were regenerated as in Fig. 4. The mixtures were kept in the dark for 20–24 h at 30 °C, and the residual absorbance was determined.

DISCUSSION

Bacteriorhodopsin was the first transmembrane protein for which a structural model containing seven membrane-spanning α -helices was proposed (6). A number of similar models has been advanced, for this protein, that differ only in the sizes of the individual helices and of the loops protruding from the lipid bilayer (7, 8). In particular, the location and size of the B-C and E-F loops in these models are based only on enzymatic digestion studies including chymotryptic cleavage (B-C loop) and photoaffinity labeling (E-F loop) (7). Other information from spin labeling and proteolysis lends further support to the loop identification (8, 30). Most recently, Henderson *et al.* (9) used electron microscopy to reconstruct a three-dimensional image of bR. Their interpretation of this image, incorporating a comprehensive body of structural data, has led to the most detailed bR model to date. This model includes atomic structures for six of the helices. Fig. 1 shows the helix and loop assignments proposed in this work (9).

What are the contributions of the individual loops shown in Fig. 1 to folding and stability? Are their lengths required for optimal helix-helix interactions in the membrane? Are any biochemical functions served by the loops? We chose to study the effect(s) of reductions in the sizes of the two larger loops (B-C and E-F) on the structure and function of bR. We created two deletions in the B-C loop and one in the E-F loop to approach the questions raised above (Fig. 1).

Each of the three deletion mutants was able to fold; however, their stabilities toward specific denaturants were found to be different. The helices pack to give reasonable rates of retinal binding (Fig. 4), form characteristic chromophores (Fig. 5), and show proton pumping (Fig. 7). The general stability, as measured by SDS and thermal denaturation was diminished in a similar way for all the mutants. The effects of deletions in the two loops differ in their influence on the stability of the retinal environment. Thus, in the B-C loop mutants, proton pumping is greatly reduced, and the chromophore is more easily accessible to hydroxylamine than in the E-F mutant.

We draw the following interpretations from our results. The basic structure of the bR molecule is not dictated by the detailed arrangement of the loop structures, but the organization of the loops contributes to stability. If the extramembranous loops were completely disordered, one would expect

that shortening them would add to the stability of the protein by reducing the entropic term in folding, since the loops connect adjacent helices in the structure. Therefore the finding of destabilization supports a more ordered loop structure. Our CD data may be interpreted as supporting helical structure in the loops. The latest structural map of bR suggests that the loop regions are compact and that they may form short extramembranous α -helices (9).

Why is there such a dramatic difference between the stability of the mutants toward hydroxylamine and their stability toward SDS? From the rate of SDS denaturation, we would conclude that the E-F mutant was more denatured; yet hydroxylamine bleaching indicates the B-C mutants are more denatured. We may account for this apparent discrepancy by noting that the hydroxylamine bleaching rate is sensitive to highly localized perturbations of the structure and the retinal environment, whereas SDS denaturation acts more generally on the structure.

The very efficient refolding of bR from the denatured state for each of the mutants shows that strong specific packing interactions between the helices are retained and play a dominant role in bR folding. Thus, even bR cleaved through the loops will refold (7, 25, 26). For these interactions to be retained in the mutants, the deletions must be wholly contained in the loops, that is, not include helix initiation regions. In particular, loop E-F must be large enough to completely contain the eight amino acids deleted, since deletion has no significant effect on refolding or proton pumping. Therefore, we would like to propose that Henderson's model (Fig. 1) should be adjusted, within his own estimated uncertainty of a few amino acids at the loop boundaries, so that Val¹⁶⁷ and Ala¹⁶⁸ are included in loop E-F. Photoaffinity labeling experiments also support this modification (7).

Acknowledgments—We are grateful to Dr. Uttam L. RajBhandary for his constructive criticisms throughout the course of this work. We appreciate Ted Kahn's assistance with the CD experiments. We thank Drs. Debra Thompson and Sabine Flitsch for their generous gifts of pure soybean and *H. halobium* lipids.

REFERENCES

- Racker, E., and Stoerkenius, W. (1974) *J. Biol. Chem.* **249**, 662–663
- Khorana, H. G., Gerber, G. E., Herlihy, W. C., Gray, C. P., Anderegg, R. J., Nihei, K., and Biemann, K. (1979) *Proc. Natl. Acad. Sci. U. S. A.* **76**, 5046–5050
- Ovchinnikov, Yu. A., Abdulaev, N. G., Feigina, M. Yu., Kiselev, A. V., and Lobanov, N. A. (1979) *FEBS Lett.* **100**, 219–224
- Dunn, R., McCoy, J., Simsek, M., Majumdar, A., Chang, S. H., RajBhandary, U. L., and Khorana, H. G. (1981) *Proc. Natl. Acad. Sci. U. S. A.* **78**, 6744–6748
- Bayley, H., Huang, K.-S., Ramachandran, R., Alonzo, H. R., Takagaki, Y., and Khorana, H. G. (1981) *Proc. Natl. Acad. Sci. U. S. A.* **78**, 2225–2229
- Engelman, D. M., Henderson, R., McLachlan, A. D., and Wallace, B. A. (1980) *Proc. Natl. Acad. Sci. U. S. A.* **77**, 2023–2027
- Huang, K.-S., Radhakrishnan, R., Bayley, H., and Khorana, H. G. (1982) *J. Biol. Chem.* **257**, 13616–13623
- Fimmel, S., Choli, T., Dencher, N. A., Buldt, G., and Wittmann-Liebold, B. (1989) *Biochim. Biophys. Acta* **978**, 231–240
- Henderson, R., Baldwin, J. M., Ceska, T. A., Zemlin, F., Beckmann, E., and Downing, K. H. (1990) *J. Mol. Biol.* **213**, 899–929
- Lo, K.-M., Jones, S. S., Hackett, N. R., and Khorana, H. G. (1984) *Proc. Natl. Acad. Sci. U. S. A.* **81**, 2285–2289
- Fuchs, R., and Blakesley, R. (1983) *Meth. Enzymol.* **100**, 2–38
- Birnboim, H. C., and Doly, J. (1979) *Nucleic Acids Res.* **7**, 1513–1523
- Horowicz, D. I., and Burke, J. F. (1981) *Nucleic Acids Res.* **9**, 2989–2998
- Wieslander, L. (1979) *Anal. Biochem.* **98**, 305–309
- McCoy, J. M., and Khorana, H. G. (1983) *J. Biol. Chem.* **258**, 8456–8461
- Guarante, L., Lauer, G., Roberts, T. M., and Ptashne, M. (1980) *Cell* **20**, 543–553
- Hanahan, D. (1983) *J. Mol. Biol.* **166**, 557–580
- Sanger, F., Nicklen, S., and Coulson, A. R. (1977) *Proc. Natl. Acad. Sci. U. S. A.* **74**, 5463–5467
- Smith, M., Leung, D. W., Gillam, S., Astell, C. R., Montgomery, D. L., and Hall, B. D. (1979) *Cell* **16**, 753–761
- Remaut, E., Tsao, H., and Fiers, W. (1983) *Gene (Amst.)* **22**, 103–113
- Karnik, S. S., Nassal, M., Doi, T., Jay, E., Sgaramella, V., and Khorana, H. G. (1987) *J. Biol. Chem.* **262**, 9255–9263
- Braiman, M., Stern, L. J., Chao, B. H., and Khorana, H. G. (1987) *J. Biol. Chem.* **262**, 9271–9276
- London, E., and Khorana, H. G. (1982) *J. Biol. Chem.* **257**, 7003–7011
- Rehorek, M., and Heyn, M. P. (1979) *Biochemistry* **18**, 4977–4983
- Popot, J.-L., Gerchman, S.-E., and Engelman, D. M. (1987) *J. Mol. Biol.* **198**, 655–676
- Liao, M.-J., and Khorana, H. G. (1984) *J. Biol. Chem.* **259**, 4194–4199
- Kimura, K., Mason, T. L., and Khorana, H. G. (1982) *J. Biol. Chem.* **257**, 2859–2867
- Oesterheld, D., Schuhmann, L., and Gruber, H. (1974) *FEBS Lett.* **44**, 257–261
- Huang, K.-S., Bayley, H., Liao, M.-J., London, E., and Khorana, H. G. (1981) *J. Biol. Chem.* **256**, 3802–3809
- Altenbach, C., Flitsch, S. L., Khorana, H. G., and Hubbell, W. L. (1989) *Biochemistry* **28**, 7806–7812